

Correlating Membrane Morphological Responses with Micellar Aggregation Behavior of Capric Acid and Monocaprin

Bo Kyeong Yoon,^{†,‡} Joshua A. Jackman,^{†,‡} Min Chul Kim,^{†,‡} Tun Naw Sut,^{†,‡} and Nam-Joon Cho^{*,†,‡,§}

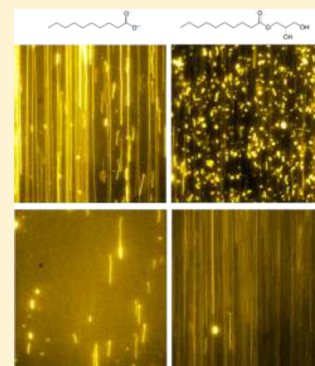
[†]School of Materials Science and Engineering, Nanyang Technological University, 50 Nanyang Avenue, 639798, Singapore

[‡]Centre for Biomimetic Sensor Science, Nanyang Technological University, 50 Nanyang Drive, 637553, Singapore

[§]School of Chemical and Biomedical Engineering, Nanyang Technological University, 62 Nanyang Drive, 637459, Singapore

Supporting Information

ABSTRACT: The interaction of single-chain lipid amphiphiles with phospholipid membranes is relevant to many scientific fields, including molecular evolution, medicine, and biofuels. Two widely studied compounds within this class are the medium-chain saturated fatty acid, capric acid, and its monoglyceride derivative, monocaprin. To date, most studies about these compounds have involved in vitro evaluation of their biological activities, while mechanistic details of how capric acid and monocaprin interact with phospholipid bilayers remain elusive. Herein, we investigated the effect of these two compounds on the morphological and fluidic properties of prefabricated, supported lipid bilayers (SLBs). The critical micelle concentration (CMC) of each compound was determined by fluorescence spectroscopy measurements. At or above its CMC, capric acid induced the formation of elongated tubules protruding from the SLB, as determined by quartz crystal microbalance-dissipation and fluorescence microscopy experiments. By contrast, monocaprin induced the formation of elongated tubules or membrane buds below and above its CMC, respectively. Fluorescence recovery after photobleaching (FRAP) experiments indicated that capric acid increased bilayer fluidity only above its CMC, whereas monocaprin increased bilayer fluidity both above and below its CMC. We discuss these findings in the context of the two compounds' structural properties, including net charge, molecular length and hydrogen-bonding capacity. Collectively, the findings demonstrate that capric acid and monocaprin differentially affect the morphological and fluidic properties of SLBs, and that the aggregation state of the compounds plays a critical role in modulating their interactions with phospholipid membranes.



INTRODUCTION

Single-chain lipid amphiphiles attract wide interest across fundamental and applied science, including fields such as molecular evolution, medicine, disinfectants and preservatives, renewable chemicals, food science, and biofuel production.^{1,2} While the lipid bilayers of biological membranes are typically composed of double-chain glycerophospholipid molecules, it is believed that biological life originated from the self-assembly of simpler building blocks such as short-chain fatty acids and monoglycerides into early cellular compartments.^{3–5} Furthermore, single-chain amphiphiles have important biological functions (e.g., antimicrobial activity, cell signaling), and are also known to interact with phospholipid bilayers, the latter of which has also inspired antimicrobial strategies aimed at destabilizing the lipid bilayers surrounding bacterial cells.^{6,7} Indeed, amidst the growing rise of antibiotic-resistant bacteria, free fatty acids and monoglycerides have emerged as promising antibacterial agents, both in the free form as preservatives and disinfectants as well as encapsulated within nanoscale drug delivery carriers as potential therapeutics.⁸ From another perspective, the interaction of phospholipid membranes with free fatty acids is also important for the fermentative production of fatty acids for renewable chemical and biofuel production because high concentrations of fatty acids can damage bacterial cell membranes.^{9,10}

For all these reasons, there is significant interest in understanding the interactions between single-chain lipid amphiphiles and phospholipid membranes.¹¹ To date, a wealth of knowledge has been obtained through antimicrobial studies which systematically investigated the influence of hydrocarbon chain properties (e.g., chain length, degrees of unsaturation) and headgroup properties on in vitro bacterial growth.^{12–14} These efforts revealed that single-chain lipid amphiphiles can damage bacterial cell membranes through either partial solubilization that hinders metabolic regulation (bacteriostatic growth inhibition) or membrane lysis (bactericidal cell death).⁶ In particular, medium-chain saturated fatty acids (between 6 and 18 carbons long) and corresponding monoglyceride derivatives were observed to have potent antibacterial effects, especially those with 10- and 12-carbon long chains.¹⁵ Lauric acid (dodecanoic acid) demonstrated broad-spectrum inhibition of Gram-positive bacteria while monolaurin (1-dodecanoyl-glycerol) was active at lower concentrations, albeit against a narrower range of bacteria.^{16,17} In marked contrast, monocaprin (1-decanoyl-glycerol) is more active against Gram-negative bacteria, especially those associated with

Received: October 31, 2016

Revised: February 13, 2017

Published: March 6, 2017

foodborne illnesses^{18,19} and it also displays virucidal activity against enveloped viruses.^{20,21} Hence, while single-chain lipid amphiphiles broadly have membrane-disruptive activities, slight differences in the physicochemical properties (e.g., chain length) can lead to dramatically different biological activities, necessitating experimental studies to delineate how these molecules differentially interact with lipid membranes.

In order to understand the morphological effects of treating bacteria, enveloped viruses, and other microorganisms with free fatty acids and monoglycerides, electron microscopy techniques have been employed for visualization of membrane damage and loss of cytoplasmic contents.^{22,23} Such experiments are conducted after treating the pathogen with high (5–10 mM) test agent concentrations followed by sample fixation.²² Atomic force microscopy has also been employed in order to investigate the morphological effects of monoglyceride treatment against bacteria.²⁴ In terms of monitoring interaction kinetics, direct measurement of the interaction between single-chain lipid amphiphiles and phospholipid membranes has been achieved using solution-based liposome assays. Specifically, the insertion of fatty acids, namely oleic acid, linoleic acid, and capric acid as well as mixtures of oleic acid and oleate, into preformed, zwitterionic phospholipid vesicles was monitored by electron microscopy and dynamic light scattering.^{25,26} In general, it was observed that fatty acid monomers incorporate into the phospholipid vesicles and form mixed fatty acid-phospholipid vesicles, inducing partial solubilization that leads to vesicle growth and subsequent fission.^{19,20} The interaction of fatty acids with giant unilamellar vesicles (GUVs) has also been reported, and it was observed that the addition of oleic acid causes GUV growth followed by formation of membrane invaginations, evaginations, and budding, resulting in the formation of small daughter vesicles.²⁷ Furthermore, Mally et al. examined the partitioning of oleic acid into GUVs, and it was noted that partitioning, in this case, increases membrane strain and results in vesicle bursting upon reaching a critical strain in the membrane.²⁸ Collectively, these studies highlight the potential of employing model membrane systems to study the dynamics of membrane-amphiphile interactions.

In particular, supported lipid bilayers (SLBs) on silicon oxide surfaces have enabled detailed mechanistic investigations by employing surface-sensitive measurement techniques.^{29,30} Thid et al. observed that the addition of a long-chain, polyunsaturated docosahexaenoic acid (DHA), at concentrations above its critical micelle concentration (CMC), induced morphological changes in the SLB, including the formation of worm-like, elongated lipid structures protruding from the bilayer.³¹ Flynn et al. have further investigated the interactions between DHA and SLBs, and noted that the specific nature of these interactions can be complex and depend on many factors such as fatty acid concentration, phospholipid composition, and the types of ions in solution.³² Recently, Yoon et al. observed that intercalation of either a medium-chain, saturated fatty acid (lauric acid) or a related anionic surfactant (sodium dodecyl sulfate) into SLBs induced membrane strain that caused the formation of protruding, worm-like tubule structures, whereas a nonionic monoglyceride (monolaurin) induced membrane budding, with the different behaviors tentatively attributed to the influence of molecular charge on membrane translocation.³³ In the same study, it was also observed that the free fatty acids and monoglycerides were appreciably more active at concentrations above their corresponding CMC values. Based on these previous investigations, there is evidence that free fatty acids

and monoglycerides induce different kinds of membrane morphological responses, although the relationship between morphological responses and the aggregation behavior of single-chain lipid amphiphiles remains to be clarified and further extended to other biologically relevant molecules in each class.

The aim of the present study is to investigate the membrane morphological responses which capric acid and monocaprin induce in SLBs, and to establish a correlation between the micellar aggregation properties of these two compounds and the resulting effects on the morphological and fluidic properties of phospholipid bilayers. Fluorescence spectroscopy was employed in order to determine the CMC values of the two compounds in appropriate solution conditions. Quartz crystal microbalance-dissipation (QCM-D) experiments were conducted in order to monitor the concentration-dependent effect of the compounds on the mass and viscoelastic properties of prefabricated SLBs, and fluorescence microscopy enabled the real-time observation of SLB morphological changes upon treatment with the two compounds. The effect of the compounds on lateral lipid diffusion within the SLB was also measured by fluorescence recovery after photobleaching (FRAP) analysis. Overall, the experimental studies reveal the influence of single-chain lipid amphiphile insertion on strain-induced membrane morphological responses as well as membrane fluidity, offering evidence that capric acid and monocaprin destabilize phospholipid membranes in different ways that depend on their corresponding molecular structure and aggregation state.

■ EXPERIMENTAL SECTION

Materials. 1,2-Dioleoyl-*sn*-glycero-3-phosphocholine (DOPC) was obtained from Avanti Polar Lipids (Alabaster, AL). Capric acid, 1-pyrene-carboxaldehyde, and sodium dodecyl sulfate were procured from Sigma-Aldrich (St Louis, MO). Monocaprin was obtained from LGC Standards (Teddington, UK). Phosphate-buffered saline (PBS) was purchased from Gibco (Carlsbad, CA). All other reagents were obtained from Sigma-Aldrich. Milli-Q-treated water (>18 M Ω -cm) (Millipore, Billerica, MA) was used for all solution preparation steps.

Preparation of Test Compound Solutions. Stock solutions of capric acid and monocaprin were first prepared by dissolving the appropriate quantity of test compound in ethanol to a final concentration of 400 mM. Then, the test compound solutions were prepared by typically diluting the stock solutions 100-fold with PBS, and the final concentration in the diluted solutions was 4 mM unless otherwise noted. In order to promote complete solubilization, the solutions were heated for 30 min at 70 °C immediately before experiment. After heating, the solutions were cooled and then further diluted to the appropriate test concentration, typically in 2-fold dilution increments. All dry compounds were stored in a dark cabinet, and samples were prepared freshly on the day of experiment.

Fluorescence Spectroscopy. Experiments were performed with a Cary Eclipse fluorescence spectrophotometer (Varian, Inc., Australia) in order to determine the critical micelle concentration of the tested compounds. Measurements were conducted at room temperature (21 °C). The fluorescence emission spectrum of the probe, 1-pyrene-carboxaldehyde, in PBS was recorded upon excitation at 365.5 nm in the presence of increasing concentrations of the test compound. To prepare the sample, a stock solution of the probe was initially prepared in methanol at a final concentration of 5 mM. A certain amount of the probe stock was added to a glass vial and left to dry for 30 min in order to fully evaporate the methanol. A PBS solution containing the appropriate amount of test compound was then added to hydrate the dried probe, followed by vortexing. The final concentration of the probe in the test solution was 0.1 μ M. All measurements for each sample were scanned six times and averaged.

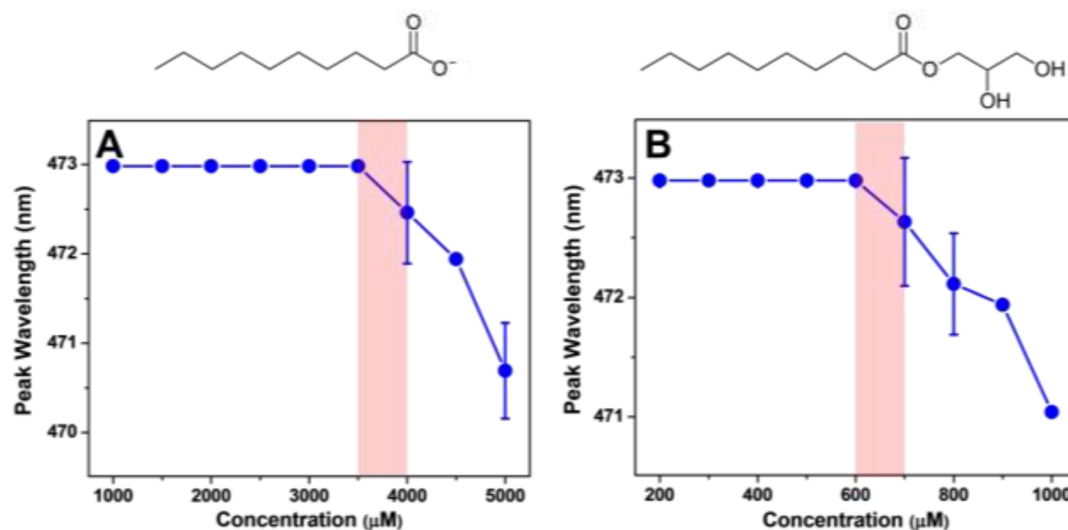


Figure 1. Determination of critical micelle concentration using the 1-pyrenecarboxaldehyde fluorescence probe. Peak wavelength is presented as a function of compound concentration in PBS solution for (A) capric acid and (B) monocaprin. The corresponding chemical structures of each compound are presented above each graph. Each data point is the average of six technical replicates ($n = 6$). The average and standard deviation (expressed as the error bars) for each data point are presented where applicable. The CMC value is defined as the highest test concentration at which no peak shift occurs.

Quartz Crystal Microbalance-Dissipation (QCM-D) Experiments. QCM-D experiments with a Q-Sense E4 instrument (Biolin Scientific, Stockholm, Sweden) were conducted in order to characterize the interaction between the test compounds and a prefabricated SLB platform. The QCM-D technique detects shifts in the resonance frequency (Δf) and energy dissipation (ΔD) of an oscillating, piezoelectric quartz crystal as a function of time, and these shifts relate to the acoustic mass and viscoelastic properties, respectively, of adsorbed biomolecules on the surface.³⁴ The sensor chips had a fundamental frequency of 5 MHz, and were coated with a sputter-coated, 50 nm-thick layer of silicon dioxide (model no. QSX 303, Biolin Scientific). The measurement data were collected at the third ($n = 3$), fifth ($n = 5$), and seventh ($n = 7$) odd overtones using the QSoft software program (Biolin Scientific), and the data was normalized according to the overtone number. Data processing was performed in the QTools (Biolin Scientific) and OriginPro 8.5 (OriginLab, Northampton, MA) software programs. All presented data was collected at the fifth overtone.

Before experiment, the chips were rinsed multiple times with water and ethanol, dried with nitrogen gas, and treated with oxygen plasma for 1 min using an Expanded Plasma Cleaner (model no. PDC-002, Harrick Plasma, Ithaca, NY). Initially, an SLB on the silicon dioxide surface was made by using the solvent-assisted lipid bilayer (SALB) method, as previously described.^{35,36} During experiments, the temperature in the measurement chamber was maintained at 25.0 ± 0.5 °C. A peristaltic pump (Reglo Digital, Ismatec, Glattbrugg, Switzerland) was used to inject liquid samples into the measurement chamber at a flow rate of $50 \mu\text{L}/\text{min}$. Each measurement set was repeated at least twice.

Fluorescence Microscopy. Epifluorescence microscopy was performed in order to directly observe morphological changes in SLBs due to treatment with capric acid or monocaprin. Experiments were conducted with an Eclipse TI-U inverted optical microscope (Nikon, Japan) with a $60\times$ magnification ($\text{NA} = 1.49$) oil-immersion objective lens (Nikon), and images were collected with an iXon 512 pixel \times 512 pixel EMCCD camera (Andor Technology, Northern Ireland). The pixel size was $0.267 \times 0.267 \mu\text{m}^2$. A fiber-coupled mercury lamp (Intensilight C-HGFIE, Nikon) was used to illuminate fluorescently labeled phospholipids with a TRITC filter. SLBs were initially formed on glass slides attached to the microfluidic flow-through chamber (sticky slide VI 0.4, Ibbidi, Germany) by using the vesicle fusion method ($0.2 \text{ mg}/\text{mL}$ extruded lipid vesicles with 72 nm average diameter). After formation, the SLB was rinsed with PBS, and

then the test compound was introduced into the measurement chamber at a flow rate of $40 \mu\text{L}/\text{min}$. Time-lapse micrographs were recorded every 5 s for a total duration of 30 min. The initial time, $t = 0$ s, was defined by when the test compound solution reached the channel inlets. The fluorescence intensity of each micrograph was normalized using a custom-written script for the Python(x,y) 2.7.5 software program.

Fluorescence Recovery after Photobleaching (FRAP) Measurements. FRAP measurements were carried out in order to monitor the lateral diffusivity of SLBs before and after treatment with the test compounds. A $20 \mu\text{m}$ diameter circular spot was photobleached for 5 s by using a 532 nm, 100 mW laser (Klaser Laser Technologies, Dortmund, Germany) and fluorescence micrographs were taken every 1 s for 90 s in total. Lateral diffusion coefficients were computed based on the Hankel transform method.³⁷

RESULTS

Determination of the Critical Micelle Concentration.

The aggregation behavior of a surface-active compound is typically characterized by the critical micelle concentration (CMC), which is defined as the lowest bulk concentration of compound at which micellar aggregates begin to form. The CMC of an amphiphilic compound can vary widely depending on its environment (e.g., solvent, ionic strength, temperature), and hence, its CMC should be determined in the appropriate solution conditions. Therefore, we determined the CMC values for capric acid and monocaprin in PBS by measuring the fluorescence emission spectrum of pyrenecarboxaldehyde in the presence of increasing concentrations of test compound.³⁸ Specifically, the 1-pyrenecarboxaldehyde probe intercalates within micelles and therefore exhibits different emission properties in the presence and absence of micelles—a spectral feature which can be utilized for determining CMC values of test compounds.³⁹ In terms of data interpretation, the peak wavelength decreases in the presence of micelles and therefore the lowest concentration of test compound which causes a decrease in the peak wavelength is defined as the CMC value.⁴⁰ Literature reports also show agreement between CMC values obtained with the fluorescence probe method and surface tension measurements.⁴⁰

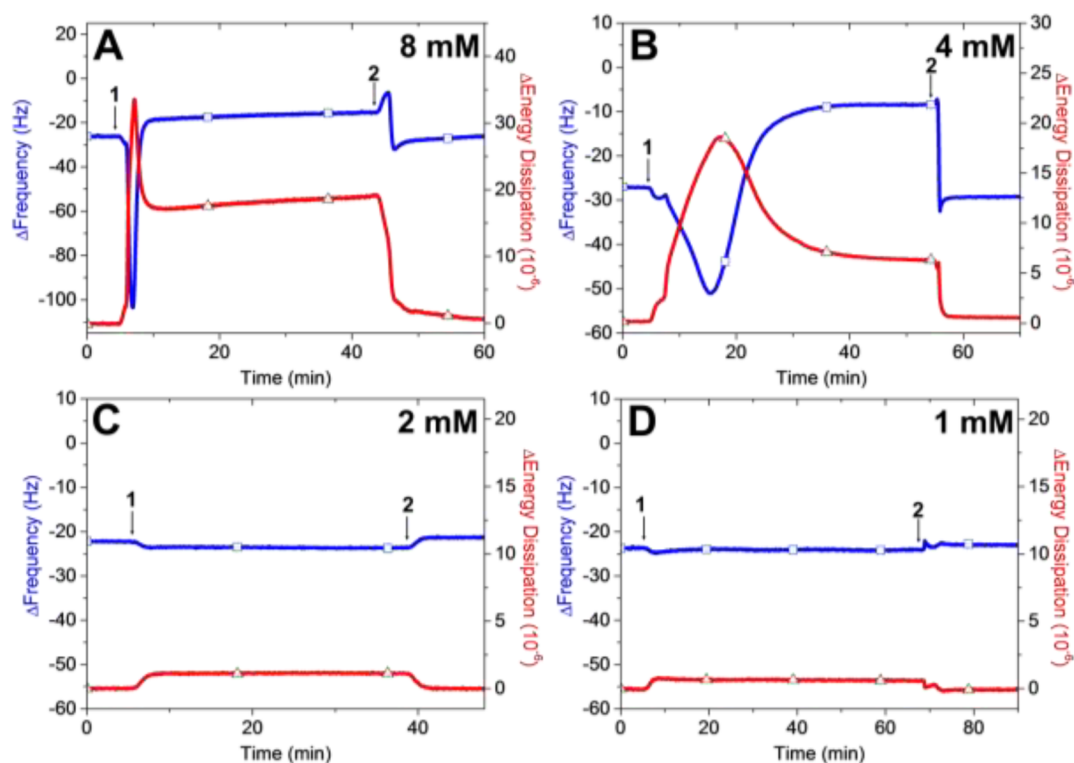


Figure 2. QCM-D investigation of capric acid treatment on supported lipid bilayers. Δf (blue line with squares) and ΔD (red line with triangles) shifts as a function of time are presented for (A) 8 mM, (B) 4 mM, (C) 2 mM, and (D) 1 mM capric acid. The initial measurement values correspond to a supported lipid bilayer on the silicon dioxide surface. Capric acid was added at $t = 5$ min (arrow 1), and a washing step was performed (arrow 2) after the measurement signals stabilized.

Before measuring the CMC values of capric acid and monocaprin, we first validated our measurement approach by characterizing the emission spectrum of the probe and testing a reference sample, SDS, with known CMC values. Upon excitation at 365.5 nm, the emission spectrum of the probe in distilled water exhibited a peak wavelength around 472 nm and there was a 1 nm redshift (473 nm) in PBS, which is consistent with previously reported empirical trends between peak wavelength and the dielectric constant of the solvent (Figure S1).^{39,41} The CMC values of SDS in distilled water and PBS were determined to be 7 mM and 800 μ M, respectively (Figure S2). The value obtained in distilled water agrees well with literature values,^{42–44} while the result obtained in PBS demonstrates how high ionic strength decreases the CMC value due to charge shielding and other molecular binding interactions.^{45,46}

Following this measurement approach, we next determined the CMC values of capric acid and monocaprin in PBS. Figure 1 presents the peak wavelength of the fluorescence emission spectrum as a function of compound concentration. The determined CMC values for capric acid and monocaprin were 3.5 mM and 600 μ M, respectively. The lower CMC value of monocaprin can be explained by its nonionic character, and hence greater propensity to aggregate, as compared to anionic fatty acid molecules. Based on these values, we designed QCM-D experiments in order to investigate how the aggregation state of capric acid and monocaprin influences the mass and viscoelastic properties of prefabricated SLBs.

Effect on Mass and Viscoelastic Properties of Supported Lipid Bilayers. In order to investigate the interaction between the test compounds and SLBs, zwitterionic SLBs composed of the 1,2-dioleoyl-*sn*-glycero-3-phosphocho-

line (DOPC) phospholipid were initially prepared on silicon dioxide-coated, QCM-D sensor chips by the solvent-assisted lipid bilayer (SALB) technique.^{35,36} The single-component DOPC lipid composition was utilized because it provides a well-controlled model membrane to probe membrane morphological responses.^{31,33} As part of the SALB procedure, a baseline signal was first obtained in aqueous buffer solution (PBS), followed by exchange to isopropanol solution, incubation in 0.5 mg/mL DOPC lipid, and finally solvent-exchange back to PBS. The formation process was characterized by the QCM-D technique, and changes in the resonance frequency (Δf) and energy dissipation (ΔD) were recorded as a function of time. The Δf and ΔD shifts reflect the mass and viscoelastic properties of the lipid layer, respectively. SLB formation was successful, as judged by final Δf and ΔD shifts of -26 ± 2 Hz and $0.3 \pm 0.2 \times 10^{-6}$, respectively. These values are in agreement with those from literature reports,⁴⁷ and indicate that the SLB is rigidly attached to the substrate with the expected areal mass density (460 ± 35 ng/cm²) as calculated by the Sauerbrey relationship which describes the relationship between the adsorbed mass and Δf shift for rigid thin films.⁴⁸

In order to determine the surface coverage of the SLB, 50 μ M bovine serum albumin (BSA) was added to bare and SLB-coated silicon dioxide surfaces. BSA adsorbs prodigiously onto silicon dioxide surfaces, but does not adsorb onto zwitterionic lipid bilayers.⁴⁹ Hence, this approach enables an estimation of bilayer surface coverage by taking into account that protein adsorption onto the bare substrate corresponds to 0% bilayer surface coverage ($\Delta f_{\text{control}}$) and assuming that reduced Δf shifts for BSA adsorption onto SLB-coated surfaces are proportional to the bilayer surface coverage. It was determined that total

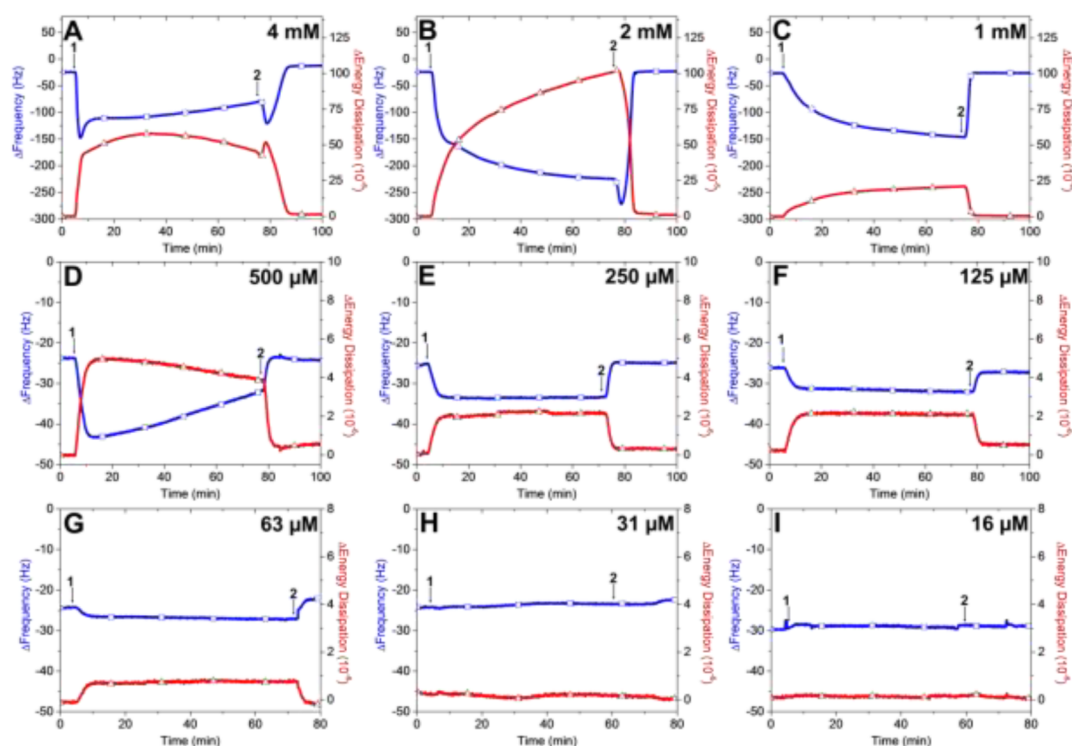


Figure 3. QCM-D investigation of monocaprin treatment on supported lipid bilayers. Δf (blue line with squares) and ΔD (red line with triangles) shifts as a function of time are presented for (A) 4 mM, (B) 2 mM, (C) 1 mM, (D) 500 μM , (E) 250 μM , (F) 125 μM , (G) 63 μM , (H) 31 μM , and (I) 16 μM monocaprin. The initial measurement values correspond to a supported lipid bilayer on the silicon dioxide surface. Monocaprin was added at $t = 5$ min (arrow 1), and a washing step was performed (arrow 2) after the measurement signals stabilized.

BSA uptake was appreciably reduced on SLB-coated surfaces (-25 Hz versus -2 Hz or less for adsorbed protein layers on bare and SLB-coated surfaces, respectively), indicating the formation of high coverage ($>93\%$) SLBs across the sensor surface (Figure S3).

After SLB fabrication and the subsequent BSA blocking step, the measurement signals were stabilized for an additional 10 min before varying concentrations of capric acid or monocaprin were added to the SLB under continuous flow conditions. The resulting changes in mass and viscoelastic properties of the SLB platform, indicative of compound binding and membrane strain-dependent morphological responses, were tracked by monitoring the Δf and ΔD shifts. The SLBs were single-use and regenerated for each individual experiment. Figures 2 and 3 present the corresponding QCM-D sensorgram results that were collected for the capric acid and monocaprin data sets. Note that the initial values of Δf and ΔD shifts at the normalized $t = 0$ min represent the values for an already formed SLB on the silicon dioxide surface.

Capric Acid. Figure 2 presents the effect of capric acid on the Δf and ΔD shifts as a function of capric acid concentration. Upon 8 mM capric acid treatment, there was a rapid decrease in Δf to around -103 Hz and increase in ΔD to 33×10^{-6} immediately after treatment (Figure 2A). After reaching inflection points, the measurement responses then began to reverse, with a rapid increase in Δf and decrease in ΔD to values of -16 Hz and 18×10^{-6} , respectively. The increase in Δf suggests that the capric acid treatment partially destabilized the SLB, along with gross morphological changes as evidenced by the large residual ΔD shift. Interestingly, when a buffer washing step was performed, a complex response in the Δf signal occurred with a net decrease to around -26 Hz whereas

the ΔD shift decreased to 0.2×10^{-6} . This behavior contrasts with previous examples of high concentrations of lauric acid treatment on SLBs, in which similar QCM-D signatures were observed for the fatty-acid–SLB interaction albeit the washing step, in that case, led to more expected measurement responses, with a net Δf increase and a net ΔD decrease.³³ As with 8 mM capric acid, a similar activity profile was observed upon treatment with 4 mM capric acid (Figure 2B). The Δf signal decreased more gradually to -52 Hz before increasing and eventually stabilizing at -9 Hz. Concurrently, the ΔD signal followed the same trend and reached an inflection point at 18×10^{-6} before decreasing again and stabilizing at 6×10^{-6} . Again, the buffer washing step, in this case, showed a steep decrease in the Δf signal and increase in the ΔD signal to final values of -29 Hz and 0.5×10^{-6} , respectively. Upon treatment with capric acid at lower concentrations (2 mM and below), there were negligible changes in both the Δf and ΔD signals of less than -2 Hz and 1×10^{-6} , respectively (Figure 2C, D). Taken together, the QCM-D results indicate that capric acid is active against SLBs when the capric acid concentration is greater than the CMC value (3.5 mM). At lower concentrations, capric acid is largely inactive against SLBs.

Monocaprin. Figure 3 presents the effect of monocaprin on the Δf and ΔD shifts as a function of monocaprin concentration. Upon treatment with 4 mM monocaprin, there was an immediate decrease in Δf to -147 Hz which occurs in parallel with a rapid increase in ΔD to 57×10^{-6} (Figure 3A). The Δf signal then decreased and eventually reached around -100 Hz before gradually increasing, while the ΔD signal reached around 50×10^{-6} before gradually decreasing. After a buffer washing step, there was a striking change in the measurement responses, yielding final Δf and ΔD

shifts of -12 Hz and 1×10^{-6} , respectively. Upon treatment with 2 mM monocaprin, even larger shifts in both Δf and ΔD were observed reaching -220 Hz and 100×10^{-6} , respectively (Figure 3B). After the buffer washing step, the final Δf and ΔD shifts returned to values around -23 Hz and 0.5×10^{-6} , respectively. A similar trend in the measurement responses was observed with treatment at 1 mM capric acid, but the maximum Δf and ΔD shifts were smaller, around -145 Hz and 20×10^{-6} , respectively (Figure 3C).

When SLBs were treated with monocaprin at lower concentrations, there were appreciably smaller measurement responses. Upon treatment with 500 μM monocaprin, there was a more moderate decrease in Δf down to -42 Hz before gradually returning to -32 Hz. The corresponding ΔD shift increased to around 4×10^{-6} (Figure 3D). A buffer washing step led to a moderate decrease in the Δf signal and sharp drop in the ΔD signal to -24 Hz and 0.5×10^{-6} , respectively. Across the concentration range of 63 to 250 μM , treatment with monocaprin resulted in progressively smaller Δf and ΔD shifts with decreasing concentration, and the measurement responses occurred quickly before stabilizing (Figure 3E–G). In these cases, buffer washing led to final Δf and ΔD values of approximately -24 Hz and 0×10^{-6} , respectively. At lower monocaprin concentrations (31 μM and below), treatment with monocaprin caused negligible Δf and ΔD shifts, indicating that monocaprin is inactive against SLBs in this low concentration range (Figure 3H, I). Collectively, at 1 mM and higher monocaprin concentrations, significant membrane morphological responses likely occurred based on the measurement responses. At intermediate concentrations between 63 and 250 μM , more moderate responses were observed, and there was negligible activity at lower concentrations. As the experimentally determined CMC value of monocaprin is 600 μM , our findings indicate that, in contrast to capric acid, monocaprin is active against SLBs at concentrations above and below its CMC value down to 63 μM . At the same time, the QCM-D measurement signatures suggest that the membrane morphological responses might differ depending on the specific monocaprin concentration, with the transition point occurring around the CMC value.

Observation of Morphological Changes in Supported Lipid Bilayers. To corroborate the QCM-D measurement signatures with specific membrane morphological responses, we performed time-lapsed fluorescence microscopy experiments which enabled direct microscopic observation of morphological changes in the SLB platform. An SLB composed of 99.5 mol % DOPC and 0.5 mol % 1,2-dipalmitoyl-*sn*-glycero-3-phosphoethanolamine-*N*-(lissamine rhodamine B sulfonyl) phospholipid was first fabricated on a silicon dioxide substrate within a microfluidic chamber. After bilayer formation, the test compound was introduced under continuous flow conditions and the resulting morphological changes were monitored with time-lapsed recording. The time point marked “ $t = 0$ min” indicated when the solution containing the test compound reached the measurement chamber. Based on the QCM-D measurement results, we tested capric acid and monocaprin at two concentrations each, one above and one below the corresponding CMC value of each compound. The tested concentrations of capric acid were 4 and 1 mM, and the concentrations of monocaprin were 1 mM and 250 μM .

Capric Acid. Figure 4 shows the time-lapsed sequence of morphological changes in an SLB upon treatment with 4 mM capric acid. Figure 4A presents the fluorescently labeled SLB,

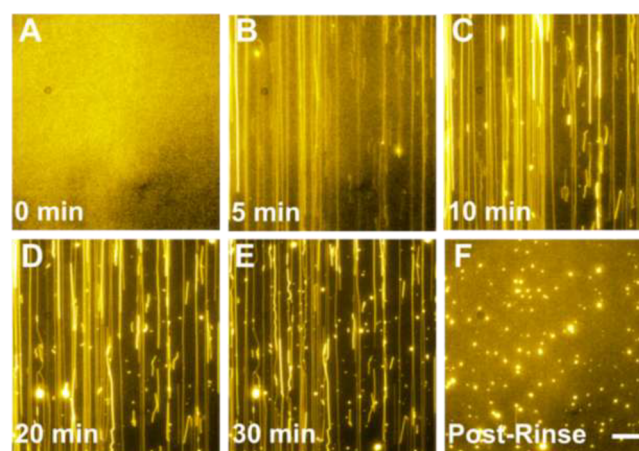


Figure 4. Microscopic observation of 4 mM capric-acid-induced tubule formation on supported lipid bilayers. (A–F) Image snapshots at various time points depict nucleation sites from which tubules grow. $t = 0$ min corresponds to the introduction of 4 mM capric acid solution into the measurement chamber. The scale bar is 20 μm .

and the introduction of capric acid caused the formation of tubules protruding from the SLB (Figure 4B). While it appears that the tubules are brighter than the SLB, this effect is likely related to the tubules being out of the focal plane of the microscope lens.⁵⁰ The tubules varied widely in length (up to 100 μm), and exhibited parallel orientation to the SLB due to the flow direction in the microfluidic channel. The elongated tubule structures remained stable under continuous flow conditions for 30 min (Figure 4C–E). Of note, the flow condition is not necessary to induce membrane morphological responses in the SLB, but it does affect the orientation of the tubules relative to the SLB. When the flow was stopped, the elongated tubule structures transitioned from a parallel orientation to a perpendicular orientation relative to the SLB (data not shown). Upon a buffer washing step, the tubules were removed and it was observed that the SLB remained underneath along with spots of bright fluorescence which appear to be nucleation sites for tubule growth (Figure 4F). The findings indicate that capric acid in the micellar form induces similar membrane morphological responses, namely the formation of elongated tubule structures, as caused by treatment with micelles of DHA³¹ and lauric acid.³³

As presented in Figure 5, the effect of 1 mM capric acid on the SLB morphological properties was also evaluated in order to determine if low concentrations of capric acid below its CMC value would still be active against SLBs. In this case, only minor activity was observed, and there was a small number of tubules formed on the SLB surface and they remained stable (Figure 5A–E). Upon buffer washing, there was negligible change in the bilayer properties aside from removal of most tubes (Figure 5F). As the experiments were conducted under continuous flow conditions, the different morphological responses observed in the 1 and 4 mM capric acid cases did not vary due to the amount of mass uptake. Rather, the evidence supports that bulk concentration of capric acid is an important factor, and the compound is appreciably more active against SLBs in the micellar form than in the monomer form. The combination of QCM-D and fluorescence microscopy results further support that capric acid in the micellar form behaves similarly to other fatty acids, including DHA and lauric

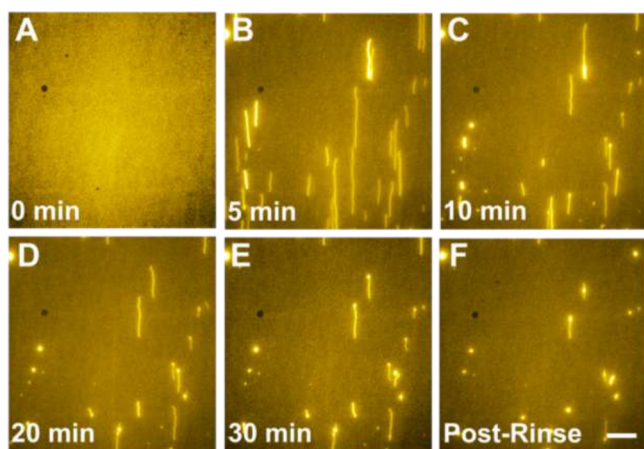


Figure 5. Microscopic observation of 1 mM capric acid addition to supported lipid bilayers. (A–F) Image snapshots at various time points during after capric acid was added to the supported lipid bilayer. The growth of a small number of tubules was observed. $t = 0$ min corresponds to the introduction of 1 mM capric acid solution into the measurement chamber. The scale bar is 20 μm .

acid, and induces the formation of elongated tubule structures protruding from SLBs.

Monocaprin. Figure 6 shows the effect of treatment of 1 mM monocaprin on SLB morphological properties.

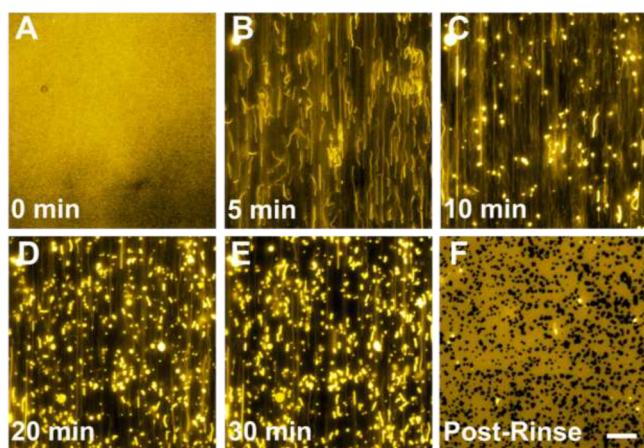


Figure 6. Microscopic observation of 1 mM monocaprin-induced bud protrusions on supported lipid bilayers. (A–F) Image snapshots at various time points depict nucleation sites from which entangled tubules grow and form buds. $t = 0$ min corresponds to the introduction of 1 mM monocaprin solution into the measurement chamber. The scale bar is 20 μm .

Initially, a large number of small tubules were formed within the first 5 min (Figure 6A). While the experiments were conducted under continuous flow conditions, it was observed that many tubules did not follow the flow orientation and instead became entangled. As time progressed, the number of tubules decreased and there was an increasing number of budlike structures that appeared within the SLB (Figure 6C–E). The buds are reminiscent of those induced by the interaction of monolaurin with SLBs, as previously reported.³³ After buffer washing, the buds and any residual tubules were removed and many defects within the SLB were apparent, as indicated by fluorophore-deficient regions (Figure 6F). Collectively, the results indicate that micellar aggregates of

monocaprin induce membrane buds resulting from entangled tubules in similar fashion to monolaurin.

As shown in Figure 7, the effect of 250 μM monocaprin on SLB morphological properties was also investigated. In marked

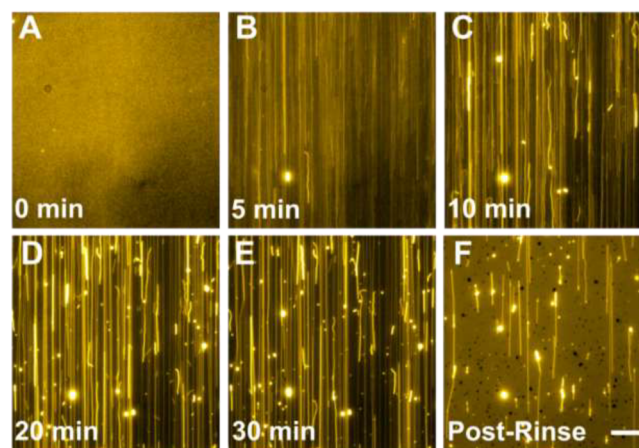


Figure 7. Microscopic observation of 250 μM monocaprin-induced tubule formation on supported lipid bilayers. (A–F) Image snapshots at various time points depict nucleation sites from which tubules grow. $t = 0$ min corresponds to the introduction of 250 μM monocaprin solution into the measurement chamber. The scale bar is 20 μm .

contrast to the capric acid case, monocaprin in the monomeric form still induced appreciable morphological changes in the SLB. Many tubules formed across the entire SLB surface and did *not* become entangled. Instead, the tubules behaved similarly to capric acid in its micellar form and nearly all the tubules formed in this case were oriented parallel to the SLB in the flow direction (Figure 7A,B). The tubules remained stable for 30 min, with only trace buds apparent (Figure 7C–E). Upon buffer washing, the majority of tubules were removed although a few tubules remained attached (Figure 7F). Importantly, many defects were also observed within the SLB after rinsing, however, they were appreciably smaller than those formed when the SLB was treated with monocaprin in the micellar form. This finding demonstrates that monocaprin in both the micellar and monomeric forms is active against SLBs, and there is a distinct transition in the resulting membrane morphological responses from elongated tubules at lower concentrations (below CMC) to membrane buds at higher concentrations (above CMC). This finding clarifies previous observations that fatty acids are active only above the corresponding CMC due to the need for micelles to provide surfactant aggregates that facilitate membrane remodeling,³¹ whereas we observe that monoglycerides, namely monocaprin, maintain some degree of activity down to 10-fold lower concentrations below the CMC.

From a broader perspective, the membrane morphological responses induced by fatty acids and monoglycerides appear to follow a spectrum of interactions whereby either elongated tubules or membrane buds can form depending on the specific conditions. As first described by Staykova et al., confined lipid bilayers regulate stress through nucleation events that result in the formation of protrusions of different geometries; with increasing membrane strain, it was noted that protrusions shift from budding cap to tubule morphologies.⁵¹ Following this morphological explanation, we observe a trend among the tested compounds, with micellar aggregates of capric acid and

monomeric monocaprin inducing greater membrane strain in SLBs than that caused by micellar aggregates of monocaprin. One important corollary observation is that monocaprin, but not capric acid, can form pore-like defects in SLBs. Monocaprin is a nonionic surfactant and, upon insertion into the lipid bilayer, can therefore translocate across leaflets on an appreciably quicker time scale than capric acid which is an anionic surfactant.⁵² As such, it is reasonable to expect that monocaprin would exhibit detergent-like membrane solubilization due to translocation across the leaflets, whereas capric acid would not do so to an appreciable extent.⁵³ In addition to large-scale morphological changes, one remaining question concerns how the membrane insertion of capric acid and monocaprin affects lateral diffusion of phospholipids within the lipid bilayer.

Effect on Lateral Lipid Diffusion. To address this question, we performed FRAP measurements in order to determine the diffusion coefficient of a fluorescently labeled phospholipid probe within the SLB before and after treatment with capric acid and monocaprin at different concentrations. As shown in Table 1, treatment with 4 mM capric acid increased

Table 1. Summary of Diffusion Coefficients Measured for Supported Lipid Bilayers before and after Treatment with Capric Acid or Monocaprin, As Determined by FRAP Measurements

treatment	D ($\mu\text{m}^2/\text{s}$)		% change
	before treatment	after treatment	
4 mM capric acid ^a	2.90 ± 0.05	3.51 ± 0.03	+21.0%
1 mM capric acid ^b	2.62 ± 0.05	2.66 ± 0.03	+1.5%
1 mM monocaprin ^a	3.04 ± 0.25	3.77 ± 0.23	+24.0%
250 μM monocaprin ^b	3.11 ± 0.07	3.64 ± 0.22	+17.0%

^aConcentration is above the corresponding CMC value. ^bConcentration is below the corresponding CMC value.

the diffusion coefficient from $2.90 \pm 0.05 \mu\text{m}^2/\text{s}$ to $3.51 \pm 0.03 \mu\text{m}^2/\text{s}$. By contrast, treatment with 1 mM capric acid had no effect as the diffusion coefficient remained similar before and after treatment. In contrast, treatment with monocaprin at both 1 mM and 250 μM concentrations led to an increase in SLB fluidity. Treatment with 1 mM monocaprin increased the diffusion coefficient from $3.04 \pm 0.25 \mu\text{m}^2/\text{s}$ to $3.77 \pm 0.23 \mu\text{m}^2/\text{s}$, while treatment with 250 μM monocaprin increased the diffusion coefficient from $3.11 \pm 0.07 \mu\text{m}^2/\text{s}$ to $3.64 \pm 0.22 \mu\text{m}^2/\text{s}$. The results demonstrate that both monomeric and micellar forms of monocaprin increase membrane fluidity whereas only micellar forms of capric acid increase membrane fluidity and monomeric capric acid has no effect.

In order to understand how these compounds increase membrane fluidity, we recall previous work by Seu et al. which demonstrated that insertion of lysophosphatidylcholine (another single-chain lipid amphiphile) into zwitterionic phospholipid SLBs also increased membrane fluidity.⁵⁴ By applying the Saffman-Delbrück model which relates lipid diffusion to membrane viscosity and height among other relevant parameters,⁵⁵ it was explained that lysophosphatidylcholine increases membrane fluidity by decreasing the bilayer height along with weakening van der Waals interactions between molecules within the bilayer because it has only one hydrocarbon chain whereas glycerophospholipids have two hydrocarbon chains. As both capric acid and monocaprin have a single, medium-length hydrocarbon chain, similar arguments

can be applied here in order to explain why these compounds increase membrane fluidity.

One last point concerns the observation that monocaprin, but not capric acid, exhibits activity in monomeric form. In general, monomeric single-chain amphiphiles are known to have short residence times within lipid bilayers.⁵⁶ Short residence times would hinder the accumulation of sufficient amounts of intercalated compound that are necessary to increase membrane strain and trigger morphological responses. Aside from the greater length of monocaprin which would likely increase residence time, another potentially important difference between capric acid and monocaprin is the capacity for hydrogen bonding with phospholipids in the lipid bilayer, which may also affect the residence time. Capric acid has a pK_a of 4.9 (ref 57) and therefore its carboxylic acid functional group is deprotonated under the experimental conditions, hence the molecule has limited potential for strong hydrogen bonding interactions with the phosphatidylcholine headgroup of DOPC molecules. By contrast, each monocaprin monomer has two $-\text{OH}$ groups that can participate in hydrogen bonding interactions (e.g., with the phosphate groups of glycerophospholipids⁵⁵) so it may have more attractive interactions with one or more phospholipids, which would increase the residence time within the bilayer, enabling intercalation of a sufficient number of molecules at a given time to cause membrane strain and membrane morphological responses. Taken together, our experimental findings indicate that monocaprin is active against SLBs at concentrations above and below its CMC value, whereas capric acid is active only at concentrations above its CMC value. These findings are consistent with the molecular features of each compound and support that a spectrum of membrane morphological responses may occur depending on the physicochemical properties of the compound as well as its aggregation state.

As mentioned in the Introduction, there is broad interest in utilizing fatty acids and monoglycerides across a wide range of applications, and both capric acid and monocaprin have been explored. In this regard, most studies empirically report the membrane-disruptive behaviors (e.g., antibacterial activity) of fatty acids and monoglycerides and there is scant discussion about the underlying interaction mechanisms or distinction between the activities of these two classes of single-chain lipid amphiphiles. Our findings support that the activities of compounds in the two classes vary and can be comparatively understood by taking into account their different physicochemical properties. Such insights suggest that membrane-active antibacterial agents likely encompass a spectrum of interactions that might work synergistically. Furthermore, the dependence of the membrane-disruptive behavior on the monomeric versus micellar aggregation state is also reminiscent of past studies on other membrane-active surfactants⁵⁸ and antibiotics⁵⁹ and applying these insights might lead to the molecular design of amphiphilic compounds with improved therapeutic profiles. All of these features should be furthered explored in the context of different application possibilities in order to build on the fundamental insights obtained in this work.

CONCLUSION

In this work, we have investigated the membrane morphological responses induced in SLBs arising from their interaction with capric acid and monocaprin, two single-chain amphiphiles of broad importance to fundamental and applied topics ranging from molecular evolution to anti-infective medicine. Fluoro-

rescence spectroscopy experiments identified the CMC values for each compound, allowing us to design a comprehensive series of QCM-D, fluorescence microscopy, and FRAP experiments that evaluated the effect of these two compounds, in the monomeric and micellar aggregation states, on the morphological and fluidic properties of SLBs. The QCM-D experiments identified that capric acid is active against SLBs only above its CMC value, whereas monocaprin is active against SLBs both above and below its CMC value. Fluorescence microscopy experiments provided morphological evidence to support the QCM-D measurement results and further demonstrated that treatment with capric acid induced the formation of tubules only above its CMC value. By contrast, treatment with monocaprin induced the formation of tubules at concentrations below its CMC value and membrane buds at concentrations above its CMC value. Furthermore, monocaprin caused detergent-like membrane solubilization across the entire range of its membrane-active concentrations, whereas capric acid did not cause membrane solubilization even at sufficiently high concentrations (above CMC) to induce tubule formation. Coupled with the differential capacities of these two compounds to influence membrane fluidity as determined by the FRAP measurements, our findings identify that capric acid and monocaprin have variable effects on the morphological and fluidic properties of phospholipid membranes, and that the aggregation state of the compounds plays a critical role in modulating their interactions with phospholipid membranes. Key factors that deserve investigation in future work include establishing a molecular-level explanation for the different membrane activities of fatty acids versus monoglycerides as well as identifying opportunities to correlate these findings in model membrane systems with physiologically relevant functions such as antibacterial activity in biological membrane systems.

■ ASSOCIATED CONTENT

Supporting Information

The Supporting Information is available free of charge on the ACS Publications website at DOI: [10.1021/acs.langmuir.6b03944](https://doi.org/10.1021/acs.langmuir.6b03944).

Critical micelle concentration determination assay and supported lipid bilayer coverage estimation (PDF)

■ AUTHOR INFORMATION

Corresponding Author

*E-mail: njcho@ntu.edu.sg.

ORCID

Nam-Joon Cho: [0000-0002-8692-8955](https://orcid.org/0000-0002-8692-8955)

Notes

The authors declare no competing financial interest.

■ ACKNOWLEDGMENTS

This work was supported by a National Research Foundation Proof-of-Concept Grant (NRF2015NRF-POC001-019) and an A*STAR-NTU-NHG Skin Research Grant (SRG/14028).

■ REFERENCES

- (1) Boyle, E.; German, J. B.; Whelan, J. Monoglycerides in membrane systems. *Crit. Rev. Food Sci. Nutr.* **1996**, *36* (8), 785–805.
- (2) Desbois, A. P. Potential applications of antimicrobial fatty acids in medicine, agriculture and other industries. *Recent Pat. Anti-Infect. Drug Discovery* **2012**, *7* (2), 111–122.

- (3) Monnard, P. A.; Deamer, D. W. Membrane self-assembly processes: Steps toward the first cellular life. *Anat. Rec.* **2002**, *268* (3), 196–207.

- (4) Olasagasti, F.; Maurel, M.-C.; Deamer, D. Physico-chemical interactions between compartment-forming lipids and other prebiotically relevant biomolecules. *BIO Web Conf.* **2014**, *2*, 05001.

- (5) Maurer, S. E.; Deamer, D. W.; Boncella, J. M.; Monnard, P.-A. Chemical evolution of amphiphiles: glycerol monoacyl derivatives stabilize plausible prebiotic membranes. *Astrobiology* **2009**, *9* (10), 979–987.

- (6) Desbois, A. P.; Smith, V. J. Antibacterial free fatty acids: activities, mechanisms of action and biotechnological potential. *Appl. Microbiol. Biotechnol.* **2010**, *85* (6), 1629–1642.

- (7) Thormar, H. *Lipids and Essential Oils as Antimicrobial Agents*; John Wiley & Sons: New York, 2011.

- (8) Jackman, J. A.; Yoon, B. K.; Li, D.; Cho, N.-J. Nanotechnology formulations for antibacterial free fatty acids and monoglycerides. *Molecules* **2016**, *21* (3), 305.

- (9) Royce, L. A.; Liu, P.; Stebbins, M. J.; Hanson, B. C.; Jarboe, L. R. The damaging effects of short chain fatty acids on *Escherichia coli* membranes. *Appl. Microbiol. Biotechnol.* **2013**, *97* (18), 8317–8327.

- (10) Royce, L. A.; Boggess, E.; Fu, Y.; Liu, P.; Shanks, J. V.; Dickerson, J.; Jarboe, L. R. Transcriptomic analysis of carboxylic acid challenge in *Escherichia coli*: beyond membrane damage. *PLoS One* **2014**, *9* (2), e89580.

- (11) Ibarguren, M.; López, D. J.; Escribá, P. V. The effect of natural and synthetic fatty acids on membrane structure, microdomain organization, cellular functions and human health. *Biochim. Biophys. Acta, Biomembr.* **2014**, *1838* (6), 1518–1528.

- (12) Kabara, J.; Vrable, R.; Jie, M. L. K. Antimicrobial lipids: natural and synthetic fatty acids and monoglycerides. *Lipids* **1977**, *12* (9), 753–759.

- (13) Kabara, J. J. Structure-function relationships of surfactants as antimicrobial agents. *J. Soc. Cosmet. Chem.* **1978**, *29*, 733–741.

- (14) Kabara, J. J. Antimicrobial agents derived from fatty acids. *J. Am. Oil Chem. Soc.* **1984**, *61* (2), 397–403.

- (15) Bergsson, G.; Steingrímsson, Ó.; Thormar, H. Bactericidal effects of fatty acids and monoglycerides on *Helicobacter pylori*. *Int. J. Antimicrob. Agents* **2002**, *20* (4), 258–262.

- (16) Kabara, J. J.; Swieczkowski, D. M.; Conley, A. J.; Truant, J. P. Fatty acids and derivatives as antimicrobial agents. *Antimicrob. Agents Chemother.* **1972**, *2* (1), 23–28.

- (17) Kabara, J. J. GRAS antimicrobial agents for cosmetic products. *J. Soc. Cosmet. Chem.* **1980**, *31*, 1–10.

- (18) Conley, A. J.; Kabara, J. J. Antimicrobial action of esters of polyhydric alcohols. *Antimicrob. Agents Chemother.* **1973**, *4* (5), 501–506.

- (19) Thormar, H.; Hilmarsson, H.; Bergsson, G. Stable concentrated emulsions of the 1-monoglyceride of capric acid (monocaprin) with microbicidal activities against the food-borne bacteria *Campylobacter jejuni*, *Salmonella spp.*, and *Escherichia coli*. *Appl. Environ. Microbiol.* **2006**, *72* (1), 522–526.

- (20) Thormar, H.; Isaacs, C.; Brown, H.; Barshatzky, M.; Pessolano, T. Inactivation of enveloped viruses and killing of cells by fatty acids and monoglycerides. *Antimicrob. Agents Chemother.* **1987**, *31* (1), 27–31.

- (21) Thormar, H.; Isaacs, C. E.; Kim, K.; Brown, H. R. Inactivation of Visna virus and other enveloped viruses by free fatty acids and monoglycerides. *Ann. N. Y. Acad. Sci.* **1994**, *724* (1), 465–471.

- (22) Bergsson, G.; Arnfinnsson, J.; Steingrímsson, Ó.; Thormar, H. Killing of Gram-positive cocci by fatty acids and monoglycerides. *APMIS* **2001**, *109* (10), 670–678.

- (23) Bergsson, G.; Arnfinnsson, J.; Steingrímsson, Ó.; Thormar, H. In vitro killing of *Candida albicans* by fatty acids and monoglycerides. *Antimicrob. Agents Chemother.* **2001**, *45* (11), 3209–3212.

- (24) Hyldegaard, M.; Sutherland, D. S.; Sundh, M.; Mygind, T.; Meyer, R. L. Antimicrobial mechanism of monocaprylate. *Appl. Environ. Microbiol.* **2012**, *78* (8), 2957–2965.

- (25) Lonchin, S.; Luisi, P. L.; Walde, P.; Robinson, B. H. A matrix effect in mixed phospholipid/fatty acid vesicle formation. *J. Phys. Chem. B* **1999**, *103* (49), 10910–10916.
- (26) Rogerson, M. L.; Robinson, B. H.; Bucak, S.; Walde, P. Kinetic studies of the interaction of fatty acids with phosphatidylcholine vesicles (liposomes). *Colloids Surf., B* **2006**, *48* (1), 24–34.
- (27) Peterlin, P.; Arrigler, V.; Kogej, K.; Svetina, S.; Walde, P. Growth and shape transformations of giant phospholipid vesicles upon interaction with an aqueous oleic acid suspension. *Chem. Phys. Lipids* **2009**, *159* (2), 67–76.
- (28) Mally, M.; Peterlin, P.; Svetina, S. a. Partitioning of oleic acid into phosphatidylcholine membranes is amplified by strain. *J. Phys. Chem. B* **2013**, *117* (40), 12086–12094.
- (29) Jackman, J. A.; Cho, N.-J.; Duran, R. S.; Frank, C. W. Interfacial binding dynamics of bee venom phospholipase A₂ investigated by dynamic light scattering and quartz crystal microbalance. *Langmuir* **2010**, *26* (6), 4103–4112.
- (30) Mechler, A.; Praporski, S.; Atmuri, K.; Boland, M.; Separovic, F.; Martin, L. L. Specific and selective peptide-membrane interactions revealed using quartz crystal microbalance. *Biophys. J.* **2007**, *93* (11), 3907–3916.
- (31) Thid, D.; Benkoski, J. J.; Svedhem, S.; Kasemo, B.; Gold, J. DHA-induced changes of supported lipid membrane morphology. *Langmuir* **2007**, *23* (11), 5878–5881.
- (32) Flynn, K. R.; Martin, L. L.; Ackland, M. L.; Torriero, A. A. Real-time quartz-crystal microbalance monitoring of free docosahexaenoic acid interactions with supported lipid bilayers. *Langmuir* **2016**, *32*, 11717–11727.
- (33) Yoon, B. K.; Jackman, J. A.; Kim, M. C.; Cho, N.-J. Spectrum of membrane morphological responses to antibacterial fatty acids and related surfactants. *Langmuir* **2015**, *31* (37), 10223–10232.
- (34) Rodahl, M.; Höök, F.; Krozer, A.; Brzezinski, P.; Kasemo, B. Quartz crystal microbalance setup for frequency and Q-factor measurements in gaseous and liquid environments. *Rev. Sci. Instrum.* **1995**, *66* (7), 3924–3930.
- (35) Tabaei, S. R.; Choi, J.-H.; Haw Zan, G.; Zhdanov, V. P.; Cho, N.-J. Solvent-assisted lipid bilayer formation on silicon dioxide and gold. *Langmuir* **2014**, *30* (34), 10363–10373.
- (36) Tabaei, S. R.; Jackman, J. A.; Kim, S.-O.; Zhdanov, V. P.; Cho, N.-J. Solvent-assisted lipid self-assembly at hydrophilic surfaces: factors influencing the formation of supported membranes. *Langmuir* **2015**, *31* (10), 3125–3134.
- (37) Jönsson, P.; Jonsson, M. P.; Tegenfeldt, J. O.; Höök, F. A method improving the accuracy of fluorescence recovery after photobleaching analysis. *Biophys. J.* **2008**, *95* (11), 5334–5348.
- (38) Kalyanasundaram, K.; Thomas, J. K. Environmental effects on vibronic band intensities in pyrene monomer fluorescence and their application in studies of micellar systems. *J. Am. Chem. Soc.* **1977**, *99* (7), 2039–2044.
- (39) Kalyanasundaram, K.; Thomas, J. K. Solvent-dependent fluorescence of pyrene-3-carboxaldehyde and its applications in the estimation of polarity at micelle-water interfaces. *J. Phys. Chem.* **1977**, *81* (23), 2176–2180.
- (40) Goddard, E.; Turro, N.; Kuo, P.; Ananthapadmanabhan, K. Fluorescence probes for critical micelle concentration determination. *Langmuir* **1985**, *1* (3), 352–355.
- (41) Turro, N. J.; Okubo, T. Polarity at the micelle-water interface under high pressure as estimated by a pyrene-3-carboxaldehyde fluorescence probe. *J. Phys. Chem.* **1982**, *86* (2), 159–161.
- (42) Benito, I.; Garcia, M.; Monge, C.; Saz, J.; Marina, M. Spectrophotometric and conductimetric determination of the critical micellar concentration of sodium dodecyl sulfate and cetyltrimethylammonium bromide micellar systems modified by alcohols and salts. *Colloids Surf., A* **1997**, *125* (2), 221–224.
- (43) Fuguet, E.; Ràfols, C.; Rosés, M.; Bosch, E. Critical micelle concentration of surfactants in aqueous buffered and unbuffered systems. *Anal. Chim. Acta* **2005**, *548* (1), 95–100.
- (44) Bhairi, S. M. *Detergents: A Guide to the Properties and Uses of Detergents in Biological Systems*; Calbiochem-Novabiochem International: San Diego, 2001.
- (45) Ambrosone, L.; Ragone, R. The interaction of micelles with added species and its similarity to the denaturant binding model of proteins. *J. Colloid Interface Sci.* **1998**, *205* (2), 454–458.
- (46) Palladino, P.; Ragone, R. Ionic strength effects on the critical micellar concentration of ionic and nonionic surfactants: The binding model. *Langmuir* **2011**, *27* (23), 14065–14070.
- (47) Cho, N.-J.; Frank, C. W.; Kasemo, B.; Höök, F. Quartz crystal microbalance with dissipation monitoring of supported lipid bilayers on various substrates. *Nat. Protoc.* **2010**, *5* (6), 1096–1106.
- (48) Sauerbrey, G. Verwendung von schwingquarzen zur wägung dünner schichten und zur mikrowägung. *Eur. Phys. J. A* **1959**, *155* (2), 206–222.
- (49) Glasmästar, K.; Larsson, C.; Höök, F.; Kasemo, B. Protein adsorption on supported phospholipid bilayers. *J. Colloid Interface Sci.* **2002**, *246* (1), 40–47.
- (50) Waters, J. C. Accuracy and precision in quantitative fluorescence microscopy. *J. Cell Biol.* **2009**, *185* (7), 1135–1148.
- (51) Staykova, M.; Arroyo, M.; Rahimi, M.; Stone, H. A. Confined bilayers passively regulate shape and stress. *Phys. Rev. Lett.* **2013**, *110* (2), 028101.
- (52) Keller, S.; Heerklotz, H.; Blume, A. Monitoring lipid membrane translocation of sodium dodecyl sulfate by isothermal titration calorimetry. *J. Am. Chem. Soc.* **2006**, *128* (4), 1279–1286.
- (53) Heerklotz, H. Interactions of surfactants with lipid membranes. *Q. Rev. Biophys.* **2008**, *41* (3–4), 205–264.
- (54) Seu, K. J.; Cambrea, L. R.; Everly, R. M.; Hovis, J. S. Influence of lipid chemistry on membrane fluidity: tail and headgroup interactions. *Biophys. J.* **2006**, *91* (10), 3727–3735.
- (55) Saffman, P.; Delbrück, M. Brownian motion in biological membranes. *Proc. Natl. Acad. Sci. U. S. A.* **1975**, *72* (8), 3111–3113.
- (56) Israelachvili, J. N. *Intermolecular and Surface Forces*, Second ed.; Academic Press: New York, 1991.
- (57) Stahl, P. H.; Wermuth, C. G. *Handbook of Pharmaceutical Salts: Properties, Selection, and Use*; John Wiley & Sons: New York, 2008.
- (58) Liu, Y.; Regen, S. L. Control over vesicle rupture and leakage by membrane packing and by the aggregation state of an attacking surfactant. *J. Am. Chem. Soc.* **1993**, *115* (2), 708–713.
- (59) Yamashita, K.; Janout, V.; Bernard, E.; Armstrong, D.; Regen, S. L. Micelle/monomer control over the membrane-disrupting properties of an amphiphilic antibiotic. *J. Am. Chem. Soc.* **1995**, *117* (23), 6249–6253.